Wire Structure Pattern Extraction and Tracking From X-Ray Images of Composites Mechanisms.

David Tschumperlé, Jalal M. Fadili, Yohan Bentolila

Wire Structure Pattern Extraction and Tracking From X-Ray Images of composite Mechanisms

D. Tschumperlé, J. Fadili
GREYC IMAGE (CNRS UMR 6072)
5 Bd Maréchal Juin, 14050 Caen Cedex, France
{David.Tschumperle, Jalal.Fadili}@greyc.ensicaen.fr

Y. Bentolila
IFP
1 et 4 rue de Bois-Préau, 92852 Rueil-Malmaison Cedex, France
Yohan.Bentolila@ifp.fr

Abstract

This paper introduces a complete pipeline of image processing methods in order to analyze and track the internal structures of a composite material. As a first step, input X-ray images are denoised, enhanced, separated into different morphological components, and geometrically filtered in order to isolate the interesting fiber inside the composite material. This requires the design of specific algorithms preserving very thin image details while being able to remove undesired image regions that may be sometimes large. For this purpose, we use state-of the-art techniques based on recent achievements in diffusion PDE's and modern harmonic analysis tools. Then, the shapes of the remaining fibered composite are individually analyzed by the use of a tensor-based tracking algorithm. We illustrate how this set of techniques allows the dynamic analysis of the composite structure when submitted to external mechanical loads.

1. Introduction and Context

Microstructure study of Composite material under stresses involves many complex mechanical phenomena and raises a strong interest in the off-shore industry [2, 5]. Composite structure used as risers are typically made of many layers. Usually composite material is made of polymer reinforced with glass or carbon fibers. Due to the use of X-ray technology, the composite fiber material has been replaced by steel in order to visualize the fiber within the composite. Fiber layers are set with opposite lay angles and are basically used to sustain tensile loads.

A way of understanding the mechanical phenomena applying on a composite part submitted to external stresses is to monitor the behavior of its various layers using an X-ray camera. For this purpose, devoted mechanical testing equipment has been developed between IFP and CEA [1] and allows to stress the composite periodically, while recording the behavior of fiber layers using a numerical X-ray video recorder (Fig. 1).

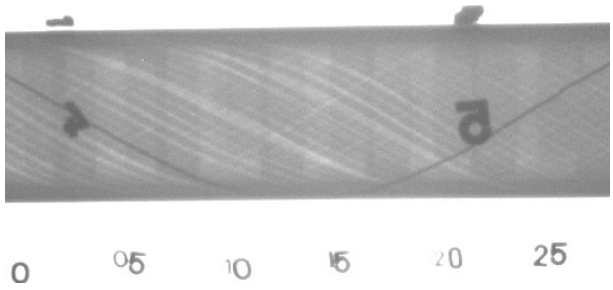

Figure 1. One of the acquired X-ray image of a composite sample.

The analysis of acquired X-ray images points out several properties which yield to develop appropriate image processing methods to extract patterns of interest. First, the used X-ray acquisition system adds non-negligible Poisson noise to the data. Second, the fiber patterns of interest have a quite low contrast while being at the same time only few pixels large. Third, black numbers corresponding to reference elements on the composite structure, hide fiber structures that exist behind them. Fourth, vertical structures are clearly visible on the image. They actually correspond to the underlying metallic frame of the experimental device and thus, it is caught by the X-ray acquisition. Last but not least, front and back layers appear as mixed in the acquired

[1] French Atomic Energy Comission (CEA).

image. This is due to the fact that the X-ray system acquires the 2D projection of the composite sample (which is initially a 3D object). This yields to a lot of cross line structures in two mainly opposite directions. With such conditions, extracting the shapes of fiber structures with accuracy in this harsh scene is a challenging goal that requires advanced image processing tools. In this paper, we propose a set of image enhancing and analysis techniques that are sequentially applied in order to track such fiber patterns in good conditions. All these methods will be illustrated on a real dataset along the article.

2. Proposed image processing pipeline

2.1. Overview of the image processing chain

As pointed out in the introduction, the data of wire structures are not directly accessible, since a lot of degradations, artefacts and information mixing are present in the acquired X-ray images.

We first tackle the denoising problem (section 2.2) by the use of a specific curvature-preserving regularization PDE, as proposed in [14]. As we want to enhance and isolate fiber structures in our images, noise removal has to be the first process to perform. It simultaneously avoids the enhancement of undesirable image structures and reduces the need of regularizing terms in image processing techniques used afterwards. In a second step, a wavelet-based image contrast enhancement (section 2.3) is applied in order to put forward fiber structures and prepare the image data for a source separation step using the so-called Morphological Component Analysis (MCA) (see section 2.4). This morphological decomposition of the image allows to clearly separate the image into two morphologically distinct components: one piece-wise smooth and the other with linear-curvilinear structures. An additional orientation filtering scheme is finally applied in order to remove vertical stripes due to the main metallic frame of the experimental device, and to separate the front and back fiber layers of the considered object (section 2.5). As a result of this image processing chain, two images are obtained corresponding to the two wire structure directions. In a last step, a fiber tracking process is performed to extract the wire pattern trajectory (section 2.6).

2.2. Image denoising

Let $I : \Omega \rightarrow \mathbb{R}$ be one of the acquired X-ray image of the considered composite. In order to remove the high amount of noise present in I, we used a technique based on regularization PDE's (partial differential equations), which are well known to be able to remove noise while preserving important discontinuities of the image data (by the mean of anisotropic filtering) [1, 7, 9, 17]. Here, important image data consist mainly in fiber structures on the composite sample. There are usually structures that are only few pixel large. In order to take this particularity into account, we use the framework of *curvature-preserving* PDE's, as proposed in [14]. We applied the following equation on the input X-ray images :

$$\frac{\partial I}{\partial t} = \text{trace}(\mathbf{TH}) + \frac{2}{\pi}\nabla I^T \int_{\alpha=0}^{\pi} \mathbf{J}_{\sqrt{\mathbf{T}}a_\alpha}\sqrt{\mathbf{T}}a_\alpha \, d\alpha \quad (1)$$

where $a_\alpha = (\cos\alpha \ \ \sin\alpha)^T$, $\mathbf{H}$ and $\mathbf{J}_{\sqrt{\mathbf{T}}a_\alpha}$ are respectively the Hessian of I and the Jacobian matrices of $\sqrt{\mathbf{T}}a_\alpha$ (matrices of the first and second spatial derivatives), while $\mathbf{T}$ is the field of 2×2 diffusion tensors :

$$\mathbf{T} = \frac{1}{(\lambda_+ + \lambda_-)^{p_+}}\theta_+\theta_+^T + \frac{1}{(\lambda_+ + \lambda_-)^{p_-}}\theta_-\theta_-^T$$

Here, λ_+, λ_- and θ_+, θ_- respectively denotes the eigenvalues and eigenvectors of the smoothed structure tensor field $\mathbf{G} = (\nabla I \nabla I^T) * G_\sigma$ [17]. User-defined parameters of the algorithm p_+ and p_- defines the local smoothing strength. This recently proposed PDE-based method has the advantage of preserving wire curved structures in the images, thanks to the constrained term $\int \mathbf{J}_{\sqrt{\mathbf{T}}a_\alpha}\sqrt{\mathbf{T}}a_\alpha$ added to the second order elliptic term $\text{trace}(\mathbf{TH})$ that basically performs a diffusion along the tensor field $\mathbf{T}$ [13, 14]. Moreover, this method can be implemented with a smart and fast numerical scheme, based on Line Integral Convolutions (as defined in [3]). It allows to perform image denoising with a sub-pixel accuracy, which is particularly well suited for our aim of image denoising with preservation of thin fiber structures. A result of our image denoising method is illustrated on Fig.2.

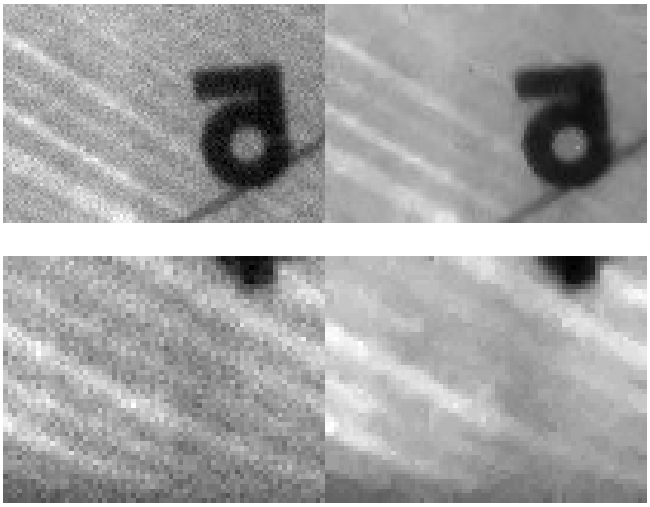

Figure 2. PDE-based denoising of X-ray images (details) : Acquired images (left), PDE-regularized images (right).

2.3. Contrast enhancement

The contrast enhancement technique that we propose is based on multiscale transforms, and more specifically on

the wavelet transform (WT). Basically, the WT can be seen as a sophisticated multi-scale differential operator that will capture the edges of the image. Then, a non-linear enhancement function is applied coefficient-wise to each wavelet sub-band, and an inverse wavelet transform is finally applied to get the enhanced image.

Several approaches have been developed in the literature for multiscale image enhancement (see e.g. [12, 6] and references therein). Here we use a non-linear global adaptive gain (GAG) function that will enhance the significant high WT coefficients and reduce the non-significant small ones (mainly due to noise). By global, we mean that the GAG function will have the same expression independently of the wavelet coefficient location. Towards this goal, the following GAG function was designed:

$$f(d'_{j,k}) = d^j_{max} a \left(\mathrm{sigm}(c(d'_{j,k} - b_j)) - \mathrm{sigm}(c(d'_{j,k} + b_j))\right) \quad (2)$$

$\mathrm{sigm(x)}$ is the sigmoid function $(1 + e^x)^{-1}$. $d'_{j,k} = d_{j,k}/d^j_{\max}$, where $d_{j,k}$ is the wavelet detail coefficient at scale j and location k, and $d^j_{\max}$ is the maximum wavelet coefficient in magnitude at scale j. c is the gain parameter (i.e. higher value of c yields more details enhancement). a and b_j are defined as follows:

$$a = \left(\mathrm{sigm}(c(1 - b_j)) - \mathrm{sigm}(c(1 + b_j))\right)^{-1}, \; b_j = \frac{T}{d^j_{\max}}$$

b_j can be thought of as a "threshold" below which the wavelet coefficients are supposed to be negligible. Therefore, a possible meaningful value would correspond to $T = \sigma\sqrt{2\log N^2}$, which is best known as the universal threshold of Donoho and Johnstone. More details can be found in [6]. The results are depicted in Fig.3, where the fine detail structures have been enhanced. Some faint structures that were hard to distinguish before this step are now clearly visible.

2.4. Source separation

Morphological Component Analysis (MCA) is a recent novel approach in modern harmonic analysis proposed by Starck et al. [11]. Its primary goal is image separation into several semantic parts (sources), where each component is sparsely represented in a given image transform. Suppose that an image I defined on a compact is a linear superposition of several parts $\{S_i\}_{i=1,\ldots,n_s}$, where each part has a parsimonious decomposition in a transform Φ_i. The union of all these transforms is usually called a (possibly hyper-) redundant dictionary. For example, if the image is composed of a piece-wise smooth part and a textured part (the so-called cartoon+texture model [16]), then two very competitive candidate transforms in the dictionary would be the wavelet transform (for the piece-wise smooth part) and the local DCT (for the locally oscillating texture).

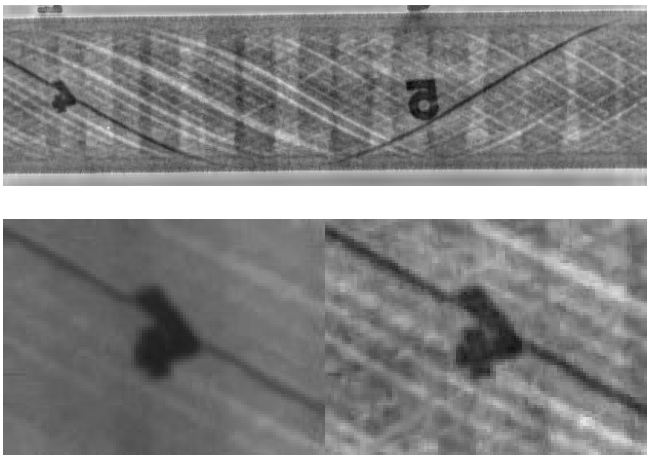

Figure 3. Effect of multi-scale contrast enhancement applied to a PDE-denoised image: top: enhanced image, bottom: zoom of an image region before (left) and after (right) enhancement.

Using both sparsity and variational mechanisms, the MCA approach attempts to solve the following optimization problem:

$$\min_{\{\alpha_i\}_{i=1,\ldots,n_s}} J(\alpha_i) = \frac{1}{2}\|X - \sum_{i=1}^{n_s} \Phi_i \alpha_i\|_2^2 + \lambda \sum_{i=1}^{n_s} \|\alpha_i\|_1 + \mu \|S_j\|_{TV}$$

Here, $S_j = \Phi_j \alpha_j$ is known to be the piecewise regular component, and $\|.\|_{TV}$ is the Total Variation norm. Penalizing with TV, will force the component S_j to be closer to a piecewise smooth image and, thus, can be helpful to support the separation process. In this formulation, beside the data fidelity term, the l_1 norm penalty on the transform coefficients promotes the sparsity of the representations.

Optimization issues In [11], the authors proposed a modification of the Block Coordinate Relaxation (BCR) algorithm to solve the above optimization problem. The interested reader may refer to [11, 10] for further details.

Candidate dictionaries Our goal is to separate the X-ray denoised and enhanced into two components: one containing the curvilinear fiber structures and the other with the lead markers appearing as black numbers in the X-ray image. These two components will be denoted hereafter S_c and S_w. Therefore, natural candidate transforms in the dictionary would be the curvelet transform [4] for S_c, which is very efficient to capture curvilinear structures, and the undecimated wavelet transform for the numbers and the piecewise constant background component S_w. The TV penalty will be added to direct the image S_w to fit the piecewise smooth model.

Fig.4 provides an illustration of the separation provided by the MCA for the above dictionaries after 30 iterations. The top row depicts the PDE-denoised and multiscale enhanced image, the middle and bottom rows give the two components S_c and S_w. The MCA performed impressively well. One can clearly see how it managed to get rid of the numbered markers while preserving the curvilinear fibers structure, and even reconstructing the unobserved fibers parts that were behind the markers.

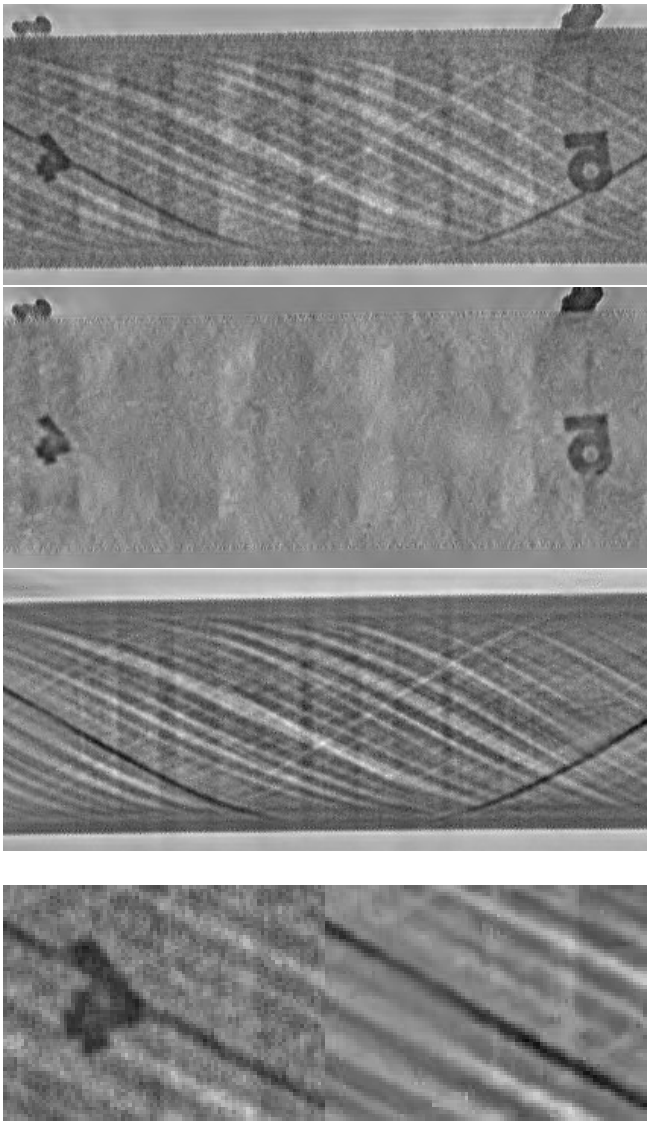

Figure 4. Results of the MCA separation step. Top row: PDE-denoised and multiscale enhanced image. Middle and bottom rows: components S_c and S_w provided by the MCA.

2.5. Orientation filtering

As stated in the introductory part, the goal of this step is twofold: (a) separate the wire structures according to their orientation in the component S_c obtained from the MCA step, (b) remove all linear structures whose main orientation is either horizontal or vertical. This amounts to a "geometrical" filtering of the component S_c. We then use the curvelet coefficients to select those coefficients that exhibit the desired geometrical (orientation) properties, and kill the others. The inverse curvelet transform is applied only to the retained coefficients to get the orientation-filtered image(s). More specifically, the component S_c is efficiently represented by the curvelet transform, and can be written as:

$$S_c(x,y) = \sum_\gamma \alpha_\gamma^c \phi_\gamma(x,y)$$

where ϕ_γ are the curvelet transform atoms indexed by their scale j, orientation θ and position (k,l) (that is $\gamma = (j,\theta,k,l)$). An orientation-filtered version of the image S_c, where all orientations are kept except θ^* can be written:

$$S_c^*(x,y) = \sum_{\gamma\in\Gamma^*} \alpha_\gamma^c \phi_\gamma(x,y)$$

where $\Gamma^* = \{(j,\theta,k,l)\ s.t.\ \theta \neq \theta^*\}$, i.e. Γ^* is the set of indices γ containing all orientations but θ^*. For example, in order to remove the horizontal and vertical structures, θ^* takes the values 0, π and $\pm\pi/2$. As far as the fiber structures are concerned, they have global orientations at $\pi/4$ and $3\pi/4$. A natural choice for the angle θ^* is obviously $\pm\pi/4$ and $\pm 3\pi/4$. However, because of classical discretization issues induced on a Cartesian grid, and also because there can be some local fluctuations on the fiber orientation, some tolerance must be allowed on θ^* to effectively remove all undesirable oriented structures. Furthermore, the number of orientations in the directional part of the curvelet transform is scale-dependent (see [4] for details). Thus, the angle tolerance on θ^* must also depend on the scale j. Formally, this corresponds to the set $\Gamma^* = \{(j,\theta,k,l)\ s.t.\ \theta \neq \theta^* \pm \Delta\theta_j^*\}$, where $\Delta\theta_j^*$ is the scale-dependent angle tolerance. In our application, we set $\Delta\theta_j = 2\pi/n_\theta^j$ where n_θ^j is the number of angular directions at scale j.
Results obtained after orientation filtering are shown in Fig.5. One important consequence of this step is that the filtered image is free from fiber structures crossings and undesired horizontal and vertical structures. This has an important impact on wire structures tracking.

2.6. Wire Structure Tracking

Having isolated the image data corresponding to interesting fiber structures on the composite, we are now able to retrieve more easily the fibers shape, since a fiber is now represented by an isovalued curve of the image pixels. Starting from an user-defined point belonging to a fiber of interest,

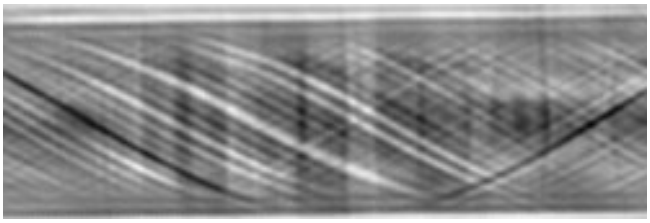

(a) Wire structures after MCA (S_c image).

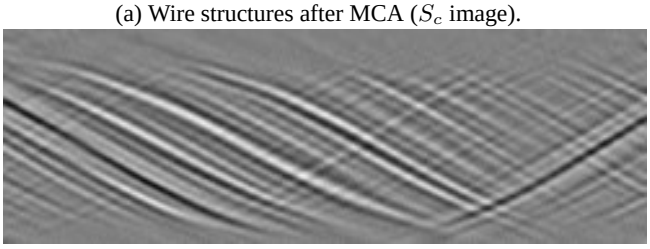

(b) Image of (a) after horizontal and vertical lines were filtered out.

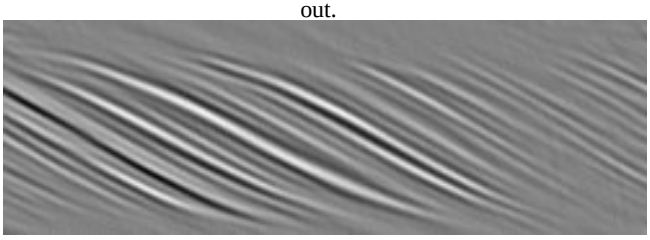

(c) Image of wire structures in the NW and SE directions.

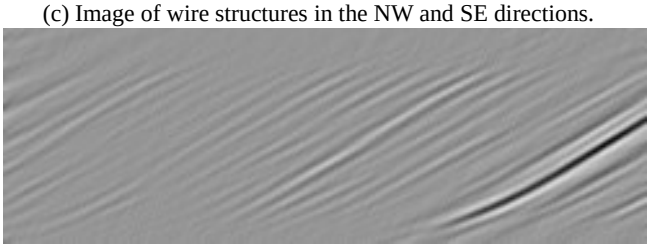

(d) Image of wire structures in the NE and SW directions.

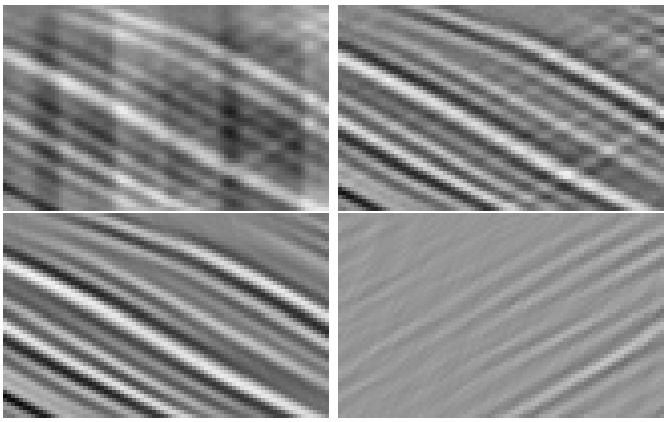

(e) Zoom of (a),(b),(c),(d).

Figure 5. Results of orientation filtering applied to the S_c MCA component.

we get its global shape by tracking the curve of constant image intensities (the color of the seed point) in both forward and backward directions. This is done by computing the integral curve of the vector field $\mathbf{w} : \mathbb{R} \rightarrow \mathbb{R}^2$ defined as the field of minimal eigenvectors of the smoothed structure tensor $\mathbf{G} = (\nabla I \nabla I^T) * G_\sigma$. This curve integration is performed through a 2nd order Runge-Kutta scheme [8]. Using this integration method allows us to find the path of minimal variations (i.e constant intensity) starting from a point , while introducing an interesting smoothness constraint on the tracked curve by the parameter σ which is the standard deviation of the structure tensor gaussian smoothing. This regularity prior is justified by the nature of the tracked object. Results of fiber tracking in one frame (back and front layers) are illustrated on Fig.6.

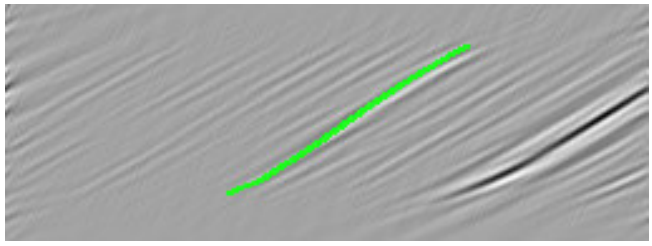

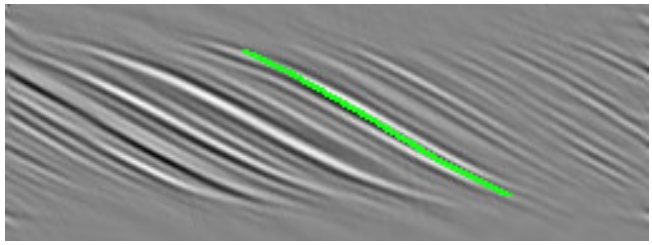

Figure 6. Result of fiber tracking on front and back layers of the composite (green line).

Our scheme is actually similar to the one used in recent works on fiber tracking in 3D volumetric images of diffusion tensor MRI [15].

Acknowledgement

The development of this image processing method has been performed within an industrial project sponsored by Technip. The authors would like to express their gratitude to Technip research and development department for facilities access and data supports.

Conclusion & Perspectives

In this paper, we combined elements from PDE-based image processing and modern harmonic analysis to provide an effective solution to a challenging and complex image pro-

cessing problem: fiber structures tracking on a composite sample observed at the output of an X-ray image acquisition system. Because of the low quality X-ray images, and many other complicating factors (e.g. projection of 3D structure onto a 2D plane), direct tracking on the original image is not possible. We then proposed to enhance the quality of the image and isolate the fiber structures prior to the fiber tracking step. Towards this goal, a curvature-preserving PDE-based approach was used for image denoising, while harmonic analysis with variational tools were proposed to enhance and separate the fiber structures. Finally, a tensor-based filamentary structure tracking algorithm was applied on the enhanced and simplified image. The obtained results are very precise and the complete pipeline of proposed image processing methods was successfully validated on a large database of composite X-ray images. Nonetheless, at this time, the tracking algorithm is still at a preliminary stage and deserves a much deeper work. Our ongoing work is directed towards this aspect.

References

[1] G. Aubert and P. Kornprobst. *Mathematical Problems in Image Processing: PDE's and the Calculus of Variations*, vol. 147 of *Applied Mathematical Sciences*.Springer-Verlag, January 2002. 2

[2] P. Odru, Y. Poirette , Y. Stassen, J.F. Saint Marcoux , L. Abergel *Composite Riser And Export Line Systems For Deep Offshore Applications.* 22nd International Conference on Offshore Mechanics and Arctic Engineering (OMAE), Cancun, Mexico June 813, 2003. 1

[3] B. Cabral, L.C. Leedom. *Imaging vector fields using line integral convolution.* Computer Graphics Proceedings, p.263–270, 1993. 2

[4] E. J. Candes, L. Demanet, D. L. Donoho and L. Ying. *Fast Discrete Curvelet Transforms*. Technical Report. CalTech. 2005. 3, 4

[5] M. Toussaint, Y. Poirette. *Composite Riser for Ultra deep Offshore: the CORFU Project.* Forth International Conference On Composite Materials For Offshore Operations, Houston, TX, October 4-6, 2005. 1

[6] T. Gessat. *Multiscale Image Contrast Enhancement*. Master Thesis. ENSI de Caen. 2003. 3

[7] P. Perona and J. Malik. *Scale-space and edge detection using anisotropic diffusion.* IEEE Transactions on Pattern Analysis and Machine Intelligence, 12(7):629–639, July 1990. 2

[8] W.H. Press, B.P. Flannery, S.A. Teukolsky, and W.T. Vetterling. *"Runge-Kutta Method"* in Numerical Recipes in FORTRAN: The Art of Scientific Computing, Cambridge University Press, pp. 704-716, 1992. 5

[9] G. Sapiro. *Geometric Partial Differential Equations and Image Analysis*. Cambridge University Press, 2001. 2

[10] S. Sardy, A. Bruce, and P. Tseng. *Block Coordinate Relaxation methods for nonparametric wavelet denoising*. Journal of Computational and Graphical Statistics, vol. 9, No 2, pp. 361-379, 2000. 3

[11] J.-L. Starck, M. Elad, and D. Donoho. *Image decomposition via the combination of sparse representations and variational approach*. IEEE Trans. Im. Proc., vol. 14, No 10, pp. 1351-1382, October 2005. 3

[12] J.-L. Starck, F. Murtagh, E. Candes, and D. Donoho. *Gray and Color Image Contrast Enhancement by the Curvelet Transform*. IEEE Trans. Im. Proc., vol. 12, No 6, pp. 706-717, June 2003. 3

[13] D. Tschumperle, R. Deriche. *Vector-Valued Image Regularization with PDE's : A Common Framework for Different Applications.* IEEE Transactions on Pattern Analysis and Machine Intelligence, vol.27, No 4, April 2005. 2

[14] D. Tschumperle. *Fast Anisotropic Smoothing of Multi-Valued Images using Curvature-Preserving PDE's.* To appear in IJCV (International Journal of Computer Vision), 2006. 2

[15] D. Tschumperle and R. Deriche. Diffusion tensor regularization with constraints preservation. In *IEEE Computer Society Conference on Computer Vision and Pattern Recognition*, Kauai Marriott, Hawaii, December 2001. 5

[16] L.A. Vese and S.J. Osher. *Modeling Textures with Total Variation Minimization and Oscillating Patterns in Image Processing.* Journal of Scientific Computing, 19(1-3), 2003, pp. 553-572. 3

[17] J. Weickert. *Anisotropic Diffusion in Image Processing*. Teubner-Verlag, Stuttgart, 1998. 2